

## Minireview

## Structural and mechanistic insight from high resolution structures of archaeal rhodopsins

Ehud M. Landau<sup>a,\*</sup>, Eva Pebay-Peyroula<sup>b</sup>, Richard Neutze<sup>c</sup><sup>a</sup>Membrane Protein Laboratory, Sealy Center for Structural Biology, and Department of Physiology and Biophysics, The University of Texas Medical Branch, 301 University Boulevard, Galveston, TX 77555-0437, USA<sup>b</sup>Institut de Biologie Structurale, UMR5075, CEA-CNRS-Université Joseph Fourier, 41 rue Jules Horowitz, F-38027 Grenoble Cedex 1, France<sup>c</sup>Department of Chemistry and Bioscience, Chalmers University of Technology, Box 462, S-40530 Gothenburg, Sweden

Received 25 August 2003; accepted 1 September 2003

First published online 1 October 2003

Edited by Gunnar von Heijne, Jan Rydström and Peter Brzezinski

**Abstract** Lipidic cubic phase-grown crystals yielded high resolution structures of a number of archaeal retinal proteins, the molecular mechanisms of which are being revealed as structures of photocycle intermediates become available. The structural basis for bacteriorhodopsin's mechanism of proton pumping is discussed, revealing a well-synchronized sequence of molecular events. Comparison with the high resolution structures of the halide pump halorhodopsin, as well as with the receptor sensory rhodopsin II, illustrates how small and localized structural changes result in functional divergence. Fundamental principles of energy transduction and sensory reception in the archaeal rhodopsins, which may have relevance to other systems, are discussed.

© 2003 Published by Elsevier B.V. on behalf of the Federation of European Biochemical Societies.

**Key words:** Archaeal rhodopsin; Lipidic cubic phase; Membrane protein; Structural dynamics; X-ray crystallography

## 1. Lipidic cubic phase crystallization of membrane proteins

The significance of membrane proteins in cellular processes cannot be overestimated. Representing approximately 25% of all gene products, these proteins reside in cell and organelle membranes and participate in transport, recognition and transduction processes that are vital to living systems. Despite enormous advances in structural biology in the last few decades, structural understanding of membrane proteins lags far behind that of soluble proteins. The major difficulty in working with membrane proteins stems from their bipolar surface properties, exhibiting hydrophilic and hydrophobic domains, which has impeded crystallization in many instances.

One conceptual and methodological innovation which has helped alleviate this impasse was to use lipidic cubic phases as 'membrane-mimetic' media for the stabilization and crystallization of membrane proteins [1]. The initial concept of the lipidic cubic phase crystallization, successfully applied to bacteriorhodopsin (bR), entails detergent solubilization and stabilization of membrane proteins in the curved bilayer of this

viscous material, free diffusion, formation of critical nuclei, and their growth to mature crystals by means of a 'feeding' mechanism [1]. A hypothetical molecular mechanism for this 'in cubo' crystallization process was recently published [2], which invokes hydrophobic mismatch as the driving force for membrane proteins to partition out of the curved cubic phase membrane and into stacked planar membranes in the crystalline phase. Further methodological developments include reconstitution of membrane patches into the cubic phase and crystallizing without detergent altogether [3], and the miniaturization and semi-automation of crystallization setups [4].

In the past few years lipidic cubic phase-grown crystals have yielded high resolution structures of the proton pump bR in the ground [5,6] and most photocycle intermediate states [7–11]; of the chloride pump halorhodopsin (hR) [12]; of sensory rhodopsin II (SRII) in the ground [13,14] and an early intermediate state [15], as well as of the complex of SRII with its cognate transducer HtrII [16]. Moreover, the lipidic cubic phase X-ray structure of a photosynthetic reaction center has also been refined to high resolution [17]. This minireview summarizes the high resolution structures of the archaeal retinal proteins (Fig. 1), and discusses the mechanistic insights gained from reaction intermediates (Fig. 2).

## 2. Bacteriorhodopsin and its photocycle intermediates: molecular mechanism of transmembrane proton pumping

As the simplest known light-driven proton pump, bR has long been regarded as a paradigm for elucidating the fundamental principles of vectorial ion transport against a transmembrane gradient. This 26 kDa retinal protein, found in the cell membrane of certain halophilic bacteria, has all the hallmarks of the hypothetical ion pump outlined in 1966 by Jardetzky [18]: an ion translocation channel; a transport site with high affinity for the ion to be transported; and an energy input which drives conformational changes, thereby switching the accessibility of the binding site from one side of the membrane to the other while lowering its ion affinity.

bR exhibits high stability and natural propensity to form 2D crystals, which made it an ideal target for electron diffraction studies. Indeed, it was the first membrane protein for which any structural model was presented almost three decades ago [19], revealing its heptahelical fold which is shared by all the archaeal rhodopsins (Fig. 1). The high resolution

\*Corresponding author. Fax: (1)-409-772 1301.

E-mail address: emlandau@utmb.edu (E.M. Landau).

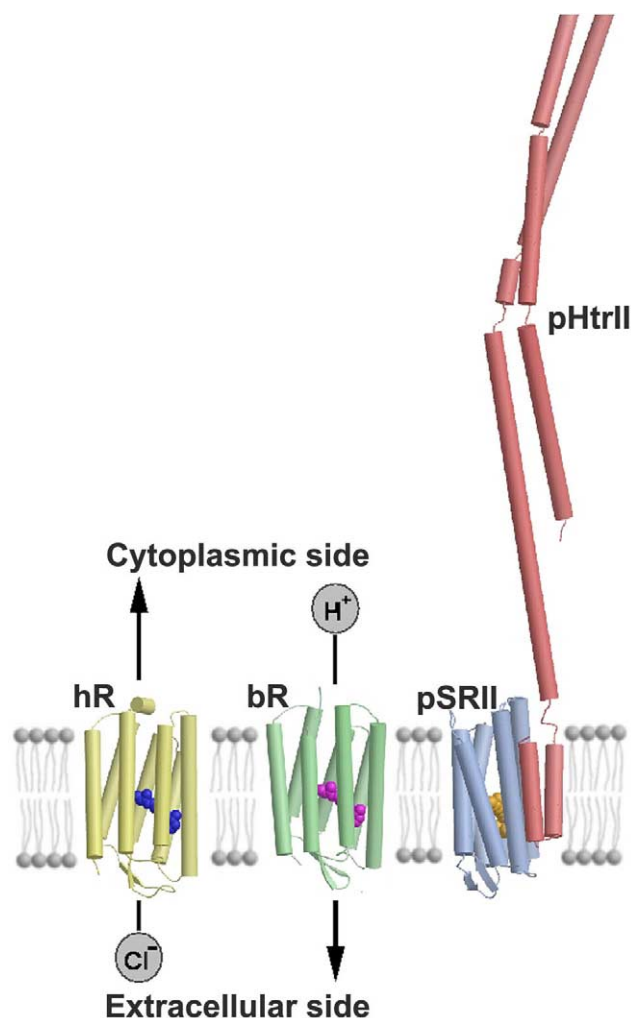


Fig. 1. Schematic representation of the archaeal rhodopsins of known crystal structure. hR [12] harvests light to pump  $\text{Cl}^-$  into the cell; bR [5] pumps protons out of the cell; and *Naerobacterium pharaonis* sensory rhodopsin II (pSRII) [13] and its cognate transducer (pHtrII) [16] initiate a negative phototaxis response in the host archaeobacterium. The X-ray structure of the cytoplasmic domain of the chemotaxis receptor [39] has been used as a structural model for the corresponding domain of HtrII in this schematic. This figure is reproduced with permission from [15].

structure of bR [5,6] reveals a proton translocation channel which is lined with a number of strategically placed charged residues and water molecules (Fig. 2). A retinal molecule covalently bound to Lys216 via a protonated Schiff base lies approximately mid-way through the membrane. From the Schiff base to the extracellular medium Asp85, Asp212, Arg82, Glu194, and Glu204 define the channel by creating a favorable polar environment for proton translocation. Together with a number of water molecules they form a continuous hydrogen-bond network from the Schiff base nitrogen to the extracellular surface. With a  $\text{pK}_a$  of 13.5 [20], the Schiff base corresponds to the high affinity proton binding site of Jardetzky. Water molecule W402 is strategically located in the active site, bridging the Schiff base and Asp85 in the ground state. In contrast, the seven  $\alpha$ -helices in bR's ground state form a compact structure from the Schiff base towards the cytoplasm. The retinal is embedded in a well-defined binding pocket sandwiched by aromatic residues that restrict the iso-

merization to the  $\text{C}_{13}=\text{C}_{14}$  double bond. Interestingly, bR in lipidic cubic phase-grown crystals exhibits a layered packing arrangement, in which trimers are ordered in a similar way to that in the purple membrane. Endogenous purple membrane lipids interact strongly with the protein, partly through hydrophobic interactions with their phytol chains, and are responsible for trimer stability and maintaining the hexagonal packing of the purple membrane.

Light activation of the chromophore results in stereospecific photoisomerization of the all-*trans*-retinal to its 13-*cis* configuration with high efficiency. Steric conflicts and charge redistribution effects initiate a sequence of conformational changes in bR which perturb the local environment of several key residues, strongly affecting their  $\text{pK}_a$  values and creating transient pathways for proton exchange. Because the absorption characteristics of the retinal are sensitive to its molecular environment, these changes can be traced spectroscopically, and define bR's photocycle, the common scheme of which is  $\text{bR}_{570} \rightarrow \text{K}_{590} \leftrightarrow \text{L}_{550} \leftrightarrow \text{M}_{412} \leftrightarrow \text{N}_{560} \leftrightarrow \text{O}_{640} \rightarrow \text{bR}_{570}$  (subscripts denote the wavelengths of room temperature absorption maxima). The key events in bR's photocycle are retinal's isomerization in the bR to K, deprotonation in the L to M, reprotonation in the M to N, and reisomerization of the retinal in the N to O transition.  $\text{M}_{412}$  is usually associated with two distinct intermediates [21], commonly referred to as the early and late M states. This spectroscopically silent transition is accompanied by a switch of the Schiff base's accessibility from the extracellular to the cytoplasmic side, thereby ensuring vectoriality of the proton pumping. In a series of papers published within 12 months of each other [7–11,22,23], several groups contributed the key ingredients towards understanding, at a structural level, how the photocycle proceeds in detail and thereby achieves vectorial proton transport. The overall picture emerging from this work was first reviewed by Kühlbrandt [24], and has since been described in detail [25]. Readers interested in the experimental conditions used in these studies, as well as the specialist tools of generating intermediate states within 3D crystals, their analysis, and correlation between X-ray crystallography and spectroscopy are referred to [25] and references therein for details.

In the ground (bR) state (inset top left, Fig. 2) X-ray studies have revealed a hydrogen-bond network which extends from the Schiff base almost to the extracellular surface [5,6]. An analogous H-bond network in the cytoplasmic side is non-existent, defining only one direction for potential proton translocation. The role of internal water molecules in the extracellular half is both structural and chemical. For example, several water molecules, particularly Wat402, help to stabilize the high proton affinity of the Schiff base [26] ( $\text{pK}_a$  of 13.5 [20]) and the low proton affinity of Asp85 ( $\text{pK}_a$  of 2.2 [27]) through H bonds to both groups in the ground state. Mutagenesis and spectroscopic studies have firmly established that Asp85 is the primary proton acceptor in bR. Structural changes are therefore necessary to remove the barrier of 11.3  $\text{pK}_a$  units prior to proton transfer from the Schiff base to Asp85. These changes must be spatially and temporally synchronized, lest bR's vectorial mode of action would be compromised.

Fourier transform infrared [28] and resonance Raman spectroscopy [29] studies have implicated that the Schiff base H bond to Wat402 is lost upon photoisomerization. This interpretation of spectra is borne out in our low temperature X-ray

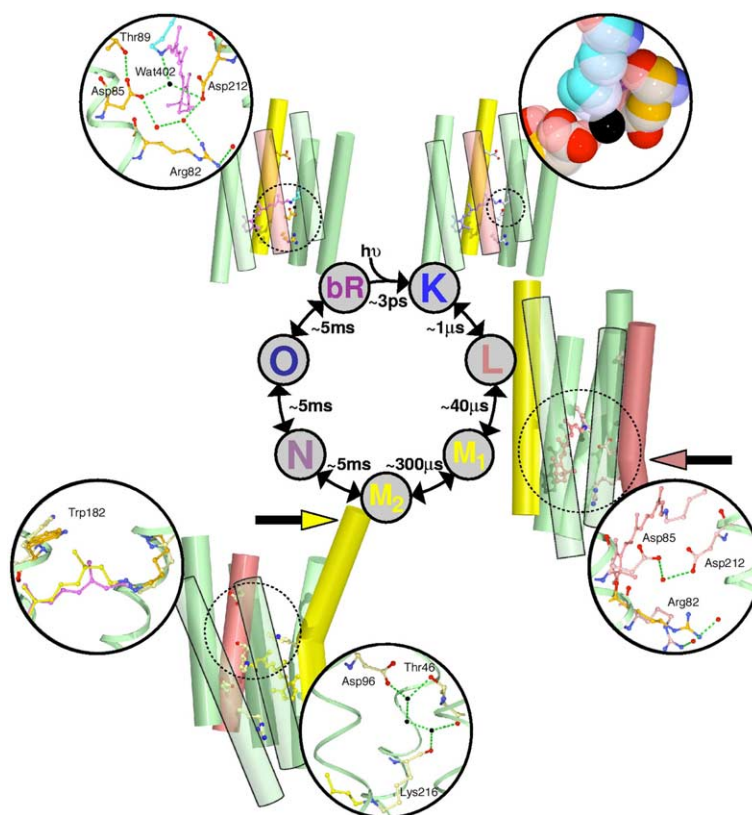


Fig. 2. Schematic representation of the major structural changes which occur during the photocycle of bR [25]. Helices are shown as green cylinders, with helix C and helix F colored red and yellow, respectively. Arrows emphasize the large conformational changes that occur in these helices. The cytoplasmic side of each representation is on top. Insets highlight the central themes discussed in the text. The H-bond network in the extracellular half is shown in the bR state (inset top left). The K-state model (inset top right) is shown in white, and is overlaid on the multi-colored ground state model, in which Wat402 is colored black. In the L state (inset bottom right) the resting state and L-state conformations of Arg82 are illustrated. The M<sub>2</sub> state illustrates ordering of water molecules, colored black, in the cytoplasmic half (inset bottom center), and steric clash between the isomerized retinal's C<sub>13</sub> methyl group and Trp182 (inset bottom left). This figure is adapted from fig. 11 of [25], and reproduced with permission.

studies of the K intermediate, since Wat402 was clearly dislocated by light activation of the retinal [7]. From the refined X-ray structure it was suggested that a steric clash with the side chain of Lys216 [25] provides a structural mechanism for the dislocation of this key water molecule (inset top right, Fig. 2). Molecular dynamics studies of the early structural changes in the photocycle of bR have led to a similar structural mechanism, with two thirds of trajectories leading to the disruption of Wat402 by the side chain of Lys216 within 80 ps [30] when using a fluctuating charge model for all water molecules.

Following the physical displacement of Wat402 a 'domino' effect results, with Wat400 and Wat401 also being disrupted and the guanidinium group of Arg82 reorienting towards the extracellular medium in the L intermediate [9,25] (inset bottom right, Fig. 2). The pK<sub>a</sub> of the Schiff base is lowered by the loss of a H bond to Wat402 [26] and the reorientation of the Schiff base N–H dipole towards a hydrophobic environment [11], whereas the pK<sub>a</sub> of Asp85 is increased due to the loss of H bonds to Thr89 and to water molecules [9], as well as the reorientation of Arg82 towards the extracellular medium. These structural changes effectively reverse the proton donor/acceptor relationship and thereby enable a proton to translocate from the Schiff base nitrogen to the carboxylate of Asp85. Formation of a well-defined, yet transient pathway for proton transfer is aided by a local bend of helix C which

brings Asp85 closer to the Schiff base in L relative to K [9,25]. This flex of a secondary structural element also explains the remarkably slow time scale for proton transfer in bR (~40 μs) and must be, at least in part, driven by the electrostatic attraction between the oppositely charged Schiff base and Asp85 (Fig. 2, bottom right). Whether the primary proton transfer step is direct [25], via Thr89 [23], or via transiently ordering water molecules [10] is unresolved, although computational methods suggest that the Schiff base proton cannot be transferred to Asp85 while a water molecule remains between these two groups [31]. Following proton transfer in the L to M transition the mutual electrostatic attraction between Asp85 and the Schiff base is cancelled, and relaxation of the retinal [23] and helix C [9,25] are postulated to draw these key groups apart, thereby hindering the reverse protonation and imposing vectoriality in the overall mechanism. Finally, the observed movement of Arg82 is suggested to destabilize the proton release group and thereby assists proton release to the extracellular medium [8].

On the cytoplasmic side, a slight rotational movement of the backbone carbonyl oxygen of Lys216 enables water molecules to transiently order in this region [32] (inset bottom center, Fig. 2), thereby creating a transient proton transfer pathway from Asp96 stretching almost as far as the Schiff base [33]. Retinal's C<sub>13</sub> methyl group comes into steric conflict with Trp182 [7] (inset bottom left, Fig. 2) which drives an

outwards tilt of helix F (bottom left, Fig. 2). The resulting large-scale displacement of  $\alpha$ -helices E, F and G of the order of 3.5 Å [22,23] exposes the cytoplasmic portion of the proton translocation channel to the bulk medium, disrupting H bonds to Asp96 [33] and perturbing its  $pK_a$ , such that a proton is first transferred from Asp96 to the Schiff base, while Asp96 is in turn reprotonated directly from the cytoplasmic medium. Reprotonation of the Schiff base accelerates the thermal reisomerization of retinal back to the all-*trans* configuration [34], eventually recovering the ground state structure as water molecules reorder and the extended H-bond network on the extracellular side reforms. This lowers the  $pK_a$  of Asp85 and, consequently, a proton moves from Asp85 to the putative proton release group. The sum of all these well-orchestrated proton transfer steps is the net translocation of a single proton from the cytoplasmic to the extracellular side of the cell membrane as a result of photoactivation, offering a conceptually similar, although somewhat more complex picture of proton translocation than that in Jardetzky's hypothetical model [18].

### 3. The archaeal rhodopsins: structural similarities and functional divergence

Certain archaeobacteria possess four light-activated retinal proteins in their cell membrane (Fig. 1): two ion pumps that mediate transmembrane energy transduction, the inwardly directed chloride pump hR, and the outwardly directed proton pump bR, as well as two photoreceptor sensory rhodopsins SRI and SRII (only SRII is illustrated in Fig. 1). Following photoexcitation, the photoreceptors undergo conformational changes and relay the light signal to their tightly bound cognate transducer proteins (HtrI and HtrII respectively), thereby initiating a phosphorylation cascade that regulates the flagellar motors of the host [35]. When oxygen and respiratory substrates are abundant, the negative phototaxis receptor SRII is expressed, allowing the host to escape potential photo-oxidative damage. In unfavorable conditions, the positive phototaxis receptor SRI is expressed and the host bacterium undergoes phototaxis to illuminated areas so as to optimize conditions. Under these circumstances bR and hR are coexpressed in large quantities and energy transduction proceeds via photosynthesis. Remarkably, SRI serves as both a positive phototaxis receptor to orange light and a negative phototaxis receptor to harmful short-wavelength radiation [35].

The archaeal rhodopsins share a common seven transmembrane  $\alpha$ -helical architecture surrounding a buried all-*trans* retinal chromophore, which is bound to a conserved lysine on helix G via a protonated Schiff base. Of this family, bR [5,6] and hR [12] from *Halobacterium salinarum*, and SRII [13,14] and the SRII:HtrII complex [16] from *Natronobacterium pharaonis* have yielded well diffracting crystals using the lipidic cubic phase method. Despite their functional diversity and ~25–30% sequence identity, they exhibit remarkably similar structures, as evidenced by a global superposition of their backbone structures. bR, hR and SRII reveal close similarity in the structure of transmembrane helices C–G, with root mean square deviation on the main chain atoms of 0.77 Å between bR and SRII, and 0.89 Å between hR and SRII [12,13], and somewhat larger deviations in helices A and B. This reinforces the notion that the pentahelical C–G fragment,

which participates in the retinal binding pocket, is strongly structurally conserved in archaeal rhodopsins [12].

hR was crystallized from the lipidic cubic phase in a similar fashion to bR [12]. The layered array of hR trimers is stacked with alternate directionality in the bilayers, with 10 lipids residing between the trimers, and three palmitates in the middle of each hR trimer. The retinal is in the all-*trans*, 15-*anti* configuration, and Thr111 and Ser115 replace Asp85 and Thr89 of bR. One chloride ion is located 3.75 Å away from the protonated Schiff base nitrogen and is ion paired thereto, as well as to Ser115. This anion is buried 18 Å beneath the membrane surface, and its solvation sphere is highly irregular. The charge distribution of the complex counter ion around the Schiff base is very similar to that of bR because the chloride ion replaces one of the negatively charged oxygen atoms of Asp85, the primary proton acceptor in bR. This chloride ion is not positioned at an angle favorable for H-bond formation with the Schiff base. This is quite distinct from structural results from the (less optimized) halide pumping D85S bR mutant, for which electron density for a bromide ion was assigned at a position directly analogous to Wat402 of bR [36]. In both studies similar structural mechanisms for halide ion transport were proposed, with the reorientation of the Schiff base N–H dipole towards the cytoplasm following retinal photoisomerization providing a driving force for the electrostatic dragging of the halide ion towards the cytoplasmic side of the protein [12,36]. The high resolution ground state structure of hR does not allow for a chloride conducting pathway between the protonated Schiff base and the cytosolic surface, and therefore light activation, and the related conformational changes must open up such a putative ion translocation pathway. This is in direct analogy with the large-scale conformational change of helices E, F and G [22,23] revealed in the later stages of the bR photocycle (Fig. 2).

In analogy with the chloride pumping mechanism of hR, these results have again raised interest in the question as to whether or not bR could be regarded as an inwardly directed hydroxide pump rather than an outwardly directed proton pump [11]. Because the net result of these two mechanisms is the same, unequivocal resolution of this question appears unlikely. However, the fact that the Schiff base deprotonation and reprotonation steps are entirely absent in the photocycles of the halide pumps but are unambiguous in bR, that a proton may be rapidly exchanged along a transient H-bond pathway with negligible energy cost, and the unlikelihood of a free hydroxide being created within the protein and surviving for a time scale of tens of  $\mu$ s, weigh in favor of the conventional picture of bR as a proton pump.

The X-ray structure of SRII from *N. pharaonis* was published independently by two groups, with resolution of 2.1 and 2.4 Å, respectively [13,14]. The protein forms crystallographic dimers, with the A and G helices at the interface, and exhibits a layered packing arrangement with alternate directionality of dimers within the plane. The retinal binding site is remarkably similar to that of bR and hR, and divides the protein into a hydrophobic cytoplasmic half and a hydrophilic extracellular half. The retinal is in the all-*trans* configuration, with the  $\beta$ -ionone ring in the 6-*s-trans* configuration. SRII is optimized to function as a negative phototaxis receptor, thus requiring that its absorption peak be tuned near the solar spectrum's maximum of 500 nm, whereas the other archaeal rhodopsins have spectral peaks at  $\lambda > 560$  nm.



Fig. 3 illustrates how the binding pocket of SRII constrains the retinal chromophore into an almost planar conformation, being somewhat less curved than retinal of bR [13]. Several factors have been suggested to play a role in the mechanism of spectral tuning. (a) The degree of retinal curvature [23]. (b) The polarity of the binding pocket near retinal's  $\beta$ -ionone ring. Significantly, all but three residues are conserved between the binding sites of bR and SRII (Fig. 3), with variations occurring on Val108, Gly130, and Thr204 in SRII (Met118, Ser141, and Ala215 respectively in bR). This is qualitatively coherent with spectral tuning effects of bR or SRII mutants involving these residues. (c) The position and orientation of the conserved Arg72 (Arg82 in bR), the guanidinium group of which is orientated toward the extracellular side of the membrane in SRII. This divergence from the conformation of Arg82 in bR has been suggested to contribute a major fraction of the observed 70 nm blue shift [14,37]. (d) The distance between Asp201 (Asp212 in bR) and the Schiff base, which was suggested to regulate the color tuning of SRII [38]. Clearly the mechanism of spectral tuning in rhodopsins is a central and complex problem, and structural results from other retinal proteins and their mutants are required should a consensus picture emerge.

The recent X-ray structure of the SRII:HtrII complex, constituting the first example of a membrane protein complex crystallized in the lipidic cubic phase, sheds new light on the mechanism of signal transduction from the photoreceptor to its cognate transducer [16]. As was previously suggested [14], Tyr199 of SRII is a key residue in forming interactions between pSRII and HtrII. A surface patch of charged and polar residues was also identified on the cytoplasmic ends of helices F and G as being unique to SRII [13]. HtrII was disordered in the region complementary to this positively charged patch and its interactions with SRII could not be assigned in the SRII:HtrII structure [16]. While a structural model for the signaling state of SRII has been built in analogy with the open conformation of bR (Fig. 2) [23], suggesting a role in signal propagation for this charged patch of residues [15], the specific details of the signal transduction await further structural models for photocycle intermediates of the SRII:HtrII complex.

Due to their structural similarity and functional diversity,

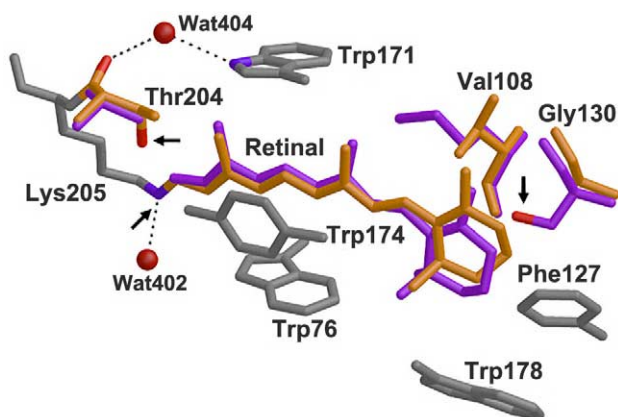


Fig. 3. Structural differences between the retinal binding pockets of bR and SRII. Retinal is colored purple (bR) and orange (SRII), conserved residues are colored gray, and varying residues are colored purple/orange. This figure is reproduced with permission from [13].

the archaeal rhodopsins have proven to be valuable model systems for elucidating several basic processes in photobiology. With the advent of the lipidic cubic phase crystallization concept [1] new possibilities for studying these molecular processes in unprecedented structural detail have arisen. These studies have revealed common themes of structural mechanism within the archaeal rhodopsin family. It is hoped that the underlying principles of energy transduction and sensory reception in the archaeal rhodopsins can be extended to advance the understanding of more complex yet functionally related processes throughout nature.

**Acknowledgements:** We would like to thank H. Belrhali, M.L. Chiu, M. Dolder, K. Edman, A. Hardmeyer, G. Katona, A. Royant, G. Rummel, and T. Ursby for experimental contributions, and S. Haacke, P. Nollert, and J.P. Rosenbusch for insightful discussions. Supported by grants from the EU-Biotech, the Swiss National Science Foundation, the Howard Hughes Medical Institute, the French Ministry of Education and Research (MENR), the Swedish Research Council (VR), and Strategic Research Foundation (SSF).

## References

- [1] Landau, E.M. and Rosenbusch, J.P. (1996) *Proc. Natl. Acad. Sci. USA* 93, 14532–14535.
- [2] Nollert, P., Qiu, H., Caffrey, M., Rosenbusch, J.P. and Landau, E.M. (2001) *FEBS Lett.* 504, 179–186.
- [3] Nollert, P., Royant, A., Pebay-Peyroula, E. and Landau, E.M. (1999) *FEBS Lett.* 457, 205–208.
- [4] Nollert, P., Navarro, J. and Landau, E.M. (2002) *Methods Enzymol.* 343, 183–199.
- [5] Belrhali, H., Nollert, P., Royant, A., Menzel, C., Rosenbusch, J.P., Landau, E.M. and Pebay-Peyroula, E. (1999) *Struct. Fold. Des.* 7, 909–917.
- [6] Luecke, H., Schobert, B., Richter, H.T., Cartailler, J.P. and Lanyi, J.K. (1999) *J. Mol. Biol.* 291, 899–911.
- [7] Edman, K., Nollert, P., Royant, A., Belrhali, H., Pebay-Peyroula, E., Hajdu, J., Neutze, R. and Landau, E.M. (1999) *Nature* 401, 822–826.
- [8] Luecke, H., Schobert, B., Richter, H.T., Cartailler, J.P. and Lanyi, J.K. (1999) *Science* 286, 255–261.
- [9] Royant, A., Edman, K., Ursby, T., Pebay-Peyroula, E., Landau, E.M. and Neutze, R. (2000) *Nature* 406, 645–648.
- [10] Sass, H.J., Buldt, G., Gessenich, R., Hehn, D., Neff, D., Schlesinger, R., Berendzen, J. and Ormos, P. (2000) *Nature* 406, 649–653.
- [11] Luecke, H. (2000) *Biochim. Biophys. Acta* 1460, 133–156.
- [12] Kolbe, M., Besir, H., Essen, L.O. and Oesterhelt, D. (2000) *Science* 288, 1390–1396.
- [13] Royant, A., Nollert, P., Edman, K., Neutze, R., Landau, E.M., Pebay-Peyroula, E. and Navarro, J. (2001) *Proc. Natl. Acad. Sci. USA* 98, 10131–10136.
- [14] Luecke, H., Schobert, B., Lanyi, J.K., Spudich, E.N. and Spudich, J.L. (2001) *Science* 293, 1499–1503.
- [15] Edman, K., Royant, A., Nollert, P., Maxwell, C.A., Pebay-Peyroula, E., Navarro, J., Neutze, R. and Landau, E.M. (2002) *Structure (Camb.)* 10, 473–482.
- [16] Gordeliy, V.I. et al. (2002) *Nature* 419, 484–487.
- [17] Katona, G., Andreasson, U., Landau, E.M., Andreasson, L.E. and Neutze, R. (2003) *J. Mol. Biol.* 331, 681–692.
- [18] Jardetzky, O. (1966) *Nature* 211, 969–970.
- [19] Henderson, R. (1975) *J. Mol. Biol.* 93, 123–138.
- [20] Sheves, M., Albeck, A., Friedman, N. and Ottolenghi, M. (1986) *Proc. Natl. Acad. Sci. USA* 83, 3262–3266.
- [21] Varo, G. and Lanyi, J.K. (1991) *Biochemistry* 30, 5008–5015.
- [22] Vonck, J. (2000) *EMBO J.* 19, 2152–2160.
- [23] Subramaniam, S. and Henderson, R. (2000) *Nature* 406, 653–657.
- [24] Kühlbrandt, W. (2000) *Nature* 406, 569–570.
- [25] Neutze, R., Pebay-Peyroula, E., Edman, K., Royant, A., Navarro, J. and Landau, E.M. (2002) *Biochim. Biophys. Acta* 1565, 144–167.

- [26] Gat, Y. and Sheves, M. (1993) *J. Am. Chem. Soc.* 115, 3772–3773.
- [27] Chang, C.H., Jonas, R., Govindjee, R. and Ebrey, T.G. (1988) *Photochem. Photobiol.* 47, 261–265.
- [28] Kandori, H., Shimono, K., Sudo, Y., Iwamoto, M., Shichida, Y. and Kamo, N. (2001) *Biochemistry* 40, 9238–9346.
- [29] Braiman, M. (1986) *Methods Enzymol.* 127, 587–597.
- [30] Hayashi, S., Tajkhorshid, E. and Schulten, K. (2002) *Biophys. J.* 83, 1281–1297.
- [31] Murata, K., Fujii, Y., Enomoto, N., Hata, M., Hoshino, T. and Tsuda, M. (2000) *Biophys. J.* 79, 982–991.
- [32] Takei, H., Gat, Y., Rothman, Z., Lewis, A. and Sheves, M. (1994) *J. Biol. Chem.* 269, 7387–7389.
- [33] Luecke, H., Schobert, B., Cartailler, J.P., Richter, H.T., Rosen-garth, A., Needleman, R. and Lanyi, J.K. (2000) *J. Mol. Biol.* 300, 1237–1255.
- [34] Balashov, S.P., Imasheva, E.S., Govindjee, R. and Ebrey, T.G. (1996) *Biophys. J.* 70, 473–481.
- [35] Spudich, J.L. (1998) *Mol. Microbiol.* 28, 1051–1058.
- [36] Facciotti, M.T., Cheung, V.S., Nguyen, D., Rouhani, S. and Glaeser, R.M. (2003) *Biophys. J.* 85, 451–458.
- [37] Ren, L., Martin, C.H., Wise, K.J., Gillespie, N.B., Luecke, H., Lanyi, J.K., Spudich, J.L. and Birge, R.R. (2001) *Biochemistry* 40, 13906–13914.
- [38] Hayashi, S., Tajkhorshid, E., Pebay-Peyroula, E., Royant, A., Landau, E.M., Navarro, J. and Schulten, K. (2001) *J. Phys. Chem. B* 105, 10124–10131.
- [39] Kim, K.K., Yokota, H. and Kim, S.H. (1999) *Nature* 400, 787–792.